

# 1,2,4,5-Tetrakis(tetramethylguanidino)benzene: Synthesis and Properties of a New Molecular Electron Donor

Anastasia Peters,<sup>[a]</sup> Elisabeth Kaifer,<sup>[a]</sup> and Hans-Jörg Himmel\*<sup>[a]</sup>

**Keywords:** Organic electron donors / Guanidines / Oxidation / Protonation

The molecular electron donor 1,2,4,5-tetrakis(tetramethylguanidino)benzene (ttmgb) was synthesised by reaction between 1,2,4,5-tetraaminobenzene and 2-chloro-1,1',3,3'-tetramethylformamidinium chloride. Protonation and oxidation of the molecule were analysed. In the course of titration of initially yellow-coloured solutions of ttmgb with HCl intense and fully reversible colour changes were observed; the di- and tetraprotonated forms are green- and blue-coloured, respectively. The tetraprotonated molecule crystallised with Cl<sup>-</sup>, and the diprotonated molecule crystallised with PF<sub>6</sub><sup>-</sup> as counterions. Oxidation, which already occurs slowly in air, was followed by CV measurements. Oxidation with I<sub>2</sub> leads to deeply green-coloured solutions, from which purple-black

crystals of (ttmgb)(I<sub>3</sub>)<sub>2</sub> of metallic appearance and a layer structure were obtained. The analysis of the molecular structure shows that the  $\pi$  system has rearranged with loss of the aromatic benzene system. Quantum chemical calculations suggest ttmgb to be an excellent two-electron donor superior even to the "organic sodium" tetraazafulvalene in the gas phase. However, in polar solvents (modelled with the CO-SMO model) the situation changes (in line with the experimental results from CV measurements), as the dication of tetraazafulvalene is considerably more solvent stabilised than [ttmgb]<sup>2+</sup>.

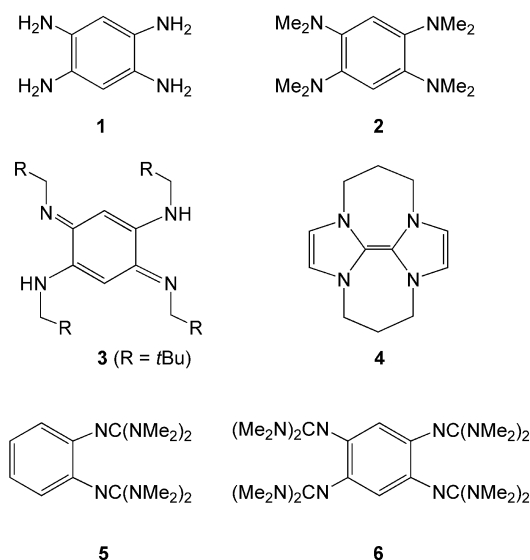
(© Wiley-VCH Verlag GmbH & Co. KGaA, 69451 Weinheim, Germany, 2009)

## Introduction

There is a long-standing interest in redox-active organic molecules. These compounds are not only of academic interest, as they are also useful for applications, for example, in preparative synthesis (especially for stoichiometric reductions) and as "noninnocent" ligands in transition-metal complexes. Some of these molecules also undergo spectacular colour changes in the course of their reactions. One important class of molecular electron donors are amino-substituted aromates. Oxidation of 1,4-bis(dimethylamino)benzene has been known since the 19th century to lead to the blue Wursters' salts.<sup>[1]</sup> 1,2,4,5-Tetraaminobenzene (**1**) is also a well-known molecule,<sup>[2]</sup> and the redox activity of its derivative 1,2,4,5-tetrakis(dimethylamino)benzene (**2**) was thoroughly studied.<sup>[3]</sup> Finally, the oxidation of hexakis(dimethylamino)benzene was assessed in several reports.<sup>[4]</sup> The analysis was extended further to other aromatic systems substituted by dimethylamino groups such as isomers of tetrakis(dimethylamino)naphthalene.<sup>[5]</sup>

Stabilisation of the oxidised form by an extended  $\pi$  system can also be found in other systems. Recently, the first examples of *N,N',N'',N'''*-tetra(alkyl)-*p*-benzoquinonedii- mines, such as **3** (with R = *t*Bu, see Scheme 1), were synthe-

sised.<sup>[6]</sup> Solutions of **3**, which itself is yellow coloured, were shown to undergo colour changes upon protonation. Hence, **3**·HCl is red coloured and **3**·2HCl is blue coloured. Moreover, in the solid state, **3**·2HCl is green coloured. It proved also possible to synthesise a first binuclear complex of **3**.<sup>[7]</sup> Furthermore, imidazole-derived donors have been used as organic super-electron donors. One representative is bisimidazolyli-dene(tetraazafulvalene) (**4**; see Scheme 1).<sup>[8]</sup> This molecule has been applied successfully for the re-



Scheme 1.

[a] Anorganisch-Chemisches Institut, Ruprecht-Karls-Universität Heidelberg, Im Neuenheimer Feld 270, 69120 Heidelberg, Germany  
Fax: +49-6221-545707  
E-mail: hans-jorg.himmel@aci.uni-heidelberg.de

Supporting information for this article is available on the WWW under <http://www.eurjoc.org> or from the author.

ductive cleavage of sulfones and sulfonamides<sup>[9]</sup> and also for the reduction of aryl iodides.<sup>[10–12]</sup> It is, however, in difference to conventional strong reducing agents such as Mg or sodium naphthenide, not capable of reducing ketones. Several other strong electron donors were also reported.<sup>[13]</sup>

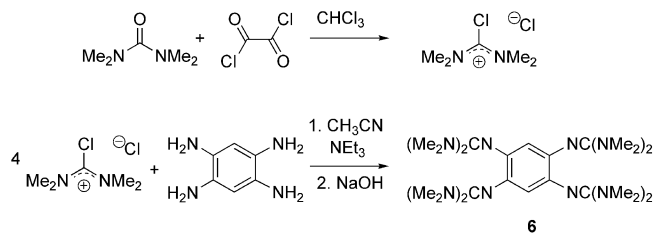
The analysis of the properties and chemistry of guanidines represents an important research theme in our group. Recently, we reported on the protonation and synthesis of several transition-metal complexes of bis(tetramethylguanidino)benzene (btmgb, **5**).<sup>[14]</sup> Here we report on the first synthesis of 1,2,4,5-tetrakis(tetramethylguanidino)benzene (ttmgb, **6**), which is a new superbasic and redox-active compound. Its oxidation and protonation will be analysed on the basis of experimental work and some quantum chemical calculations.

## Results and Discussion

This section is divided into four parts. We first report on the synthesis and characterisation of **6**. The analysis of its protonation and oxidation follows. Finally, we compare the electron donor strength with other known organic super-electron donors with the help of quantum chemical calculations.

### Synthesis and Characterisation of 1,2,4,5-Tetrakis-(tetramethylguanidino)benzene (ttmgb, **6**)

The synthesis of **6** was accomplished as sketched in Scheme 2. Reaction between 2-chloro-1,1',3,3'-tetramethylformamidinium chloride (freshly prepared from tetramethylurea and oxalyl chloride) and 1,2,4,5-tetraaminobenzene afforded the protonated product, which, after treatment with NaOH, gave **6** in 61% yield. The <sup>1</sup>H NMR spectrum of **6** showed one signal due to the protons of the methyl groups at  $\delta = 2.63$  ppm. It was shown previously in the case of other guanidines that low temperatures are necessary to freeze the various fluxional processes (rotation around the C–N and C=N bonds and possibly also pyramidal inversion at the N atoms) of the guanidino groups.<sup>[15,16]</sup> Colourless crystals of **6** were grown from CH<sub>3</sub>CN solutions and exhibit a diamond-like appearance pointing to a large refraction index. Figure 1 displays the molecular structure of **6** as determined by X-ray diffraction. Table S1 (see Supporting Information) contains selected structural parameters. The molecule possesses a centre of inversion in the solid state. With values of 139.79(17) (C1–C3') and 140.87(17) pm (C1–C2), the C–C distances within the benzene ring deviate only slightly from the C–C distance in benzene. As anticipated, the N1–C4 and N4–C9 bond lengths together with the symmetry-equivalent N1'–C4' and N4'–C9' bond lengths [128.77(16) and 129.10(16) pm] are shorter than all other guanidine C–N distances in the molecule, which is in line with their formulation as N=C bonds. For comparison, in compound **5** (see Scheme 1), N=C bond lengths of 129.1(3) and 130.1(3) pm were measured.<sup>[13]</sup>



Scheme 2.

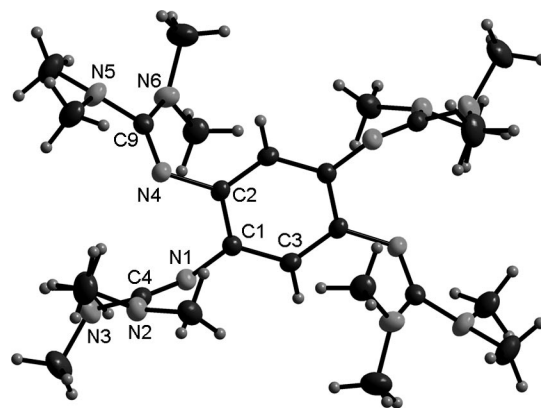


Figure 1. Molecular structure of **6**. Ellipsoids are drawn at the 50% probability level.

Figure 2 displays the UV/Vis spectrum of **6** in hexane. The UV/Vis spectrum of **5** is also included for comparison. A relatively intense electron-excitation band occurs at 329 nm ( $\epsilon = 1.36 \times 10^4$  L mol<sup>-1</sup> cm<sup>-1</sup>), which is redshifted by about 37 nm with respect to the corresponding band of **5** (292 nm).

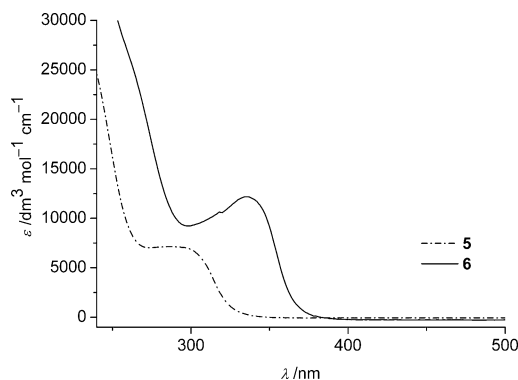


Figure 2. UV/Vis spectra of hexane solutions of **5** and **6**.

### Protonation Experiments

An aqueous 5.6 mM solution of **6** exhibited a pH value of 11.6, showing that **6** is indeed a strong base. The solution was titrated with 0.1 M HCl, and the resulting curve is plotted in Figure 3. Starting with a yellow solution of **6** (see inserted photos in Figure 3) two poorly resolved protonation steps can be observed upon addition of one and two

equivalents of HCl. After addition of two equivalents of HCl the solution exhibits a pH value of 8.6 and is thus still basic. Interestingly, the solution is green coloured at this point. Further addition of HCl leads first to a much slower decline in the pH value, showing that solutions of the diprotonated molecule have some buffer capacity. A sharp drop in the pH value is again observed upon addition of more than three equivalents of HCl. At the same time, the colour of the solution turns bright blue (see Figure 3). After addition of four equivalents of HCl the pH value is already below 3. Further addition of HCl leads to bleaching of the solution. All these colour changes are fully reversible.

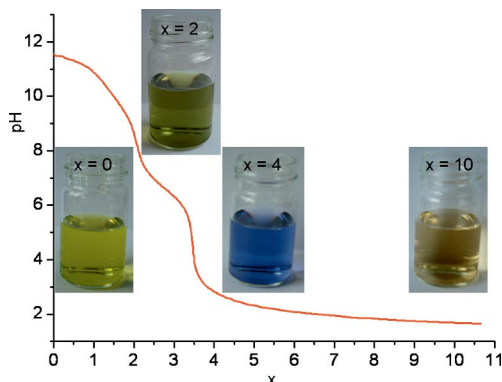


Figure 3. Titration curve for **6** with 0.1 M HCl ( $x$  being the added mol equivalents of HCl). In addition, the colours of the solutions at some stages of the curve are shown.

Pale-blue-coloured crystals of  $[\mathbf{6H}_4]\text{Cl}_4 \cdot 9\text{H}_2\text{O}$  were grown from a  $\text{CH}_3\text{CN}$  solution of **6** containing four equivalents of HCl. The molecular structure of the cationic part, which again exhibits an inversion centre, is illustrated in Figure 4. Selected structural parameters are provided in Table S2 (see Supporting Information). Protonation occurs exclusively at the four imine N atoms. The C–C distances within the benzene ring are equal to 139.30(13) and 139.24(12) pm and do not differ significantly from those in neutral **6**. Thus, the aromatic benzene ring is preserved in the course of protonation. In the  $^1\text{H}$  NMR spectrum a signal at  $\delta = 6.66$  ppm can be assigned to the two protons directly attached to the  $\text{C}_6$  ring. With values of 140.82(12) and 142.05(12) pm the C1–N1 and C2–N4 bond lengths (together with the symmetry equivalent two bond lengths) are virtually equal to those in neutral **6**. All other C–N bonds, however, change upon protonation. Thus, the N1–C4 and N4–C9 bond lengths increase from 128.77(16) and 129.10(16) pm in neutral **6** to values of 136.18(12) and 135.52(13) pm in  $[\mathbf{6H}_4]\text{Cl}_4$ . On the other hand, the C4–N2, C4–N3, C9–N5 and C9–N6 bond lengths decrease upon protonation. This argues for delocalisation of the positive charge through  $\pi$  interactions over all three C–N bonds in each guanidino unit. This delocalisation ideally requires a planar N1C4N2N3 and N4C9N5N6 unit. Indeed, the angle sums around the C4 and C9 atoms are almost perfectly  $360^\circ$  both in **6** and in  $[\mathbf{6H}_4]\text{Cl}_4$ . Four of the crystal  $\text{H}_2\text{O}$  molecules interact through  $\text{NH}\cdots\text{OH}$  hydrogen bonds [ $\text{N}\cdots\text{O}$  dis-

tances of 284.0(14) and 283.8(1) pm and estimated  $\text{NH}\cdots\text{OH}$  distances of 196.4(14) and 199.6(20) pm] with the  $[\mathbf{6H}_4]^{4+}$  unit. Furthermore, C–H $\cdots$ Cl contacts and of course O–H $\cdots$ Cl hydrogen bonds are established.

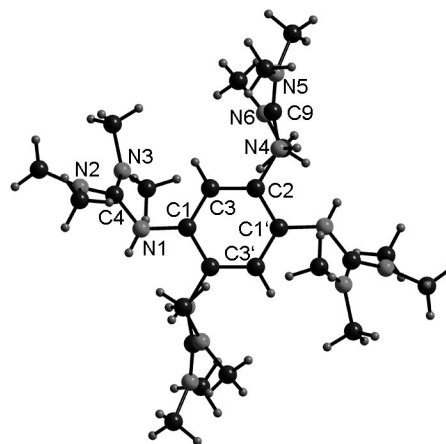


Figure 4. Molecular structure of  $(\mathbf{6H}_4)\text{Cl}_4 \cdot 9\text{H}_2\text{O}$ . Ellipsoids are drawn at the 50% probability level.

Crystals of the diprotonated form were not obtained with  $\text{Cl}^-$  but with  $\text{PF}_6^-$  as counterions. The molecular structure of one  $\mathbf{6H}_2^{2+}$  dication of  $[\mathbf{6H}_2](\text{PF}_6)_2 \cdot 1.5\text{H}_2\text{O}$  as derived from the X-ray diffraction analysis is shown in Figure 5. Table S3 in the Supporting Information contains selected structural parameters. Protonation again occurs at the imine N atoms (N4 and the symmetry equivalent N4' atom). The N1–C4 bond length remains short at 130.0(3) pm, whereas the N4–C9 bond length is elongated to 134.2(4) pm. The C9–N5 and C9–N6 bond lengths [134.6(4) and 132.8(4) pm] are significantly shorter than the C4–N2 and C4–N3 bond lengths [137.3(4) and 137.4(3) pm]. These values again indicate delocalisation of the positive charge within the two protonated guanidino units. The C–C distances within the  $\text{C}_6$  ring [139.6(4) and 139.1(4) pm] show that the aromaticity is not affected by protonation, which is in agreement with the results obtained for the tetraprotonated molecule. As anticipated, the chemical shift of the signal in the  $^1\text{H}$  NMR spectrum due

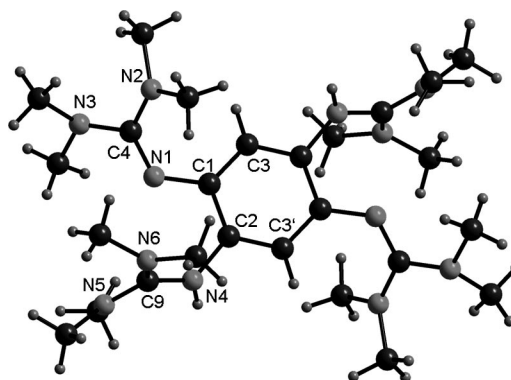


Figure 5. Molecular structure of  $[\mathbf{6H}_2](\text{PF}_6)_2 \cdot 2\text{H}_2\text{O}$ . Ellipsoids are drawn at the 50% probability level.

to the two protons directly attached to the C<sub>6</sub> ring ( $\delta = 6.11$  ppm) is in between that observed for the nonprotonated ( $\delta = 5.54$  ppm) and the tetraprotonated ( $\delta = 6.66$  ppm) molecule. The molecules form sheets in the crystalline phase. One of these sheets is sketched in Figure 6, which now also displays the disordered PF<sub>6</sub><sup>-</sup> units and the O atoms of the crystal water. The water O atoms establish O⋯H–N hydrogen bonds with the [6H<sub>2</sub>]<sup>2+</sup> units that are 212.4(3.8) pm in length.

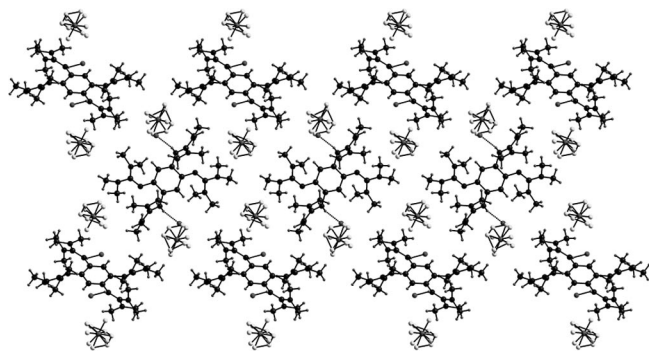


Figure 6. Packing of a sheet of [6H<sub>2</sub>](PF<sub>6</sub>)<sub>2</sub>·2H<sub>2</sub>O molecules in the solid state. Ellipsoids are drawn at the 50% probability level. Of the H<sub>2</sub>O units only the O atoms are displayed.

### Oxidation

If solutions of **6** are exposed to air for several hours or days, colour changes can be observed, signalling the occurrence of a slow redox reaction with the air O<sub>2</sub> (see below). This result already demonstrates the electron-donor capacity of **6**. The CV curve obtained for solutions of **6** in CH<sub>3</sub>CN showed a two-electron wave at  $E_{1/2}(\text{CH}_3\text{CN}) = -0.32$  V vs. SCE. Although this value is larger than the value reported for **4**,<sup>[17]</sup> it shows the potential use of **6** as a mild reducing agent. The quantum chemical calculations discussed below will shed further light on the origin of the differences in the reduction power between **4** and **6**.

Oxidation of **6** can also easily be accomplished with I<sub>2</sub>. Upon addition of I<sub>2</sub> to a solution of **6** in CH<sub>3</sub>CN, a deep-green-coloured solution was obtained, from which purple-black-coloured crystals of a metal-like appearance precipitated. These crystals turned out to be composed of 6(I<sub>3</sub>)<sub>2</sub>. The molecular structure of one of the 6(I<sub>3</sub>)<sub>2</sub> units, again featuring an inversion centre, is illustrated in Figure 7 (see Table S4 in the Supporting Information for selected structural parameters). Interestingly, the crystal exhibits a layer structure as sketched in Figure 8 (only the C<sub>6</sub> rings of each 6<sup>2+</sup> dication is shown for the sake of clarity); the C<sub>6</sub> ring planes are tilted with respect to these layers. In clear contrast to the structures of **1**<sup>2+</sup> and **2**<sup>2+</sup>,<sup>[3]</sup> the C<sub>6</sub> ring in 6<sup>2+</sup> remains planar, because the tetramethylguanidino groups can better evade one another than the dimethylamino groups. However, the C–C bond lengths within this ring vary significantly after oxidation. Whereas the C1–C2 bond length [136.3(4) pm] is shorter than that in **6** before oxidation, the C2'–C3 [142.5(4) pm] is slightly larger and the

C1–C3 distance [149.1(4) pm] is significantly larger. The change in the C<sub>6</sub> ring manifests itself also in a considerable low-field shift (by 0.37 ppm) of the signal in the <sup>1</sup>H NMR spectrum due to the two protons attached to the ring. The C<sub>9</sub>, N<sub>4</sub> and C<sub>3</sub> atoms are almost located in the benzene ring plane, whereas the N1–C4 bond points out of this plane. Consequently, the C3–N4 distance [130.4(4) pm] is shorter than the C1–N1 distance [135.6(4) pm], because the coplanarity of the C<sub>9</sub>–N<sub>4</sub>–C<sub>3</sub> group favours  $\pi$  bonding. In Scheme 3 two of several possible mesomeric structures are shown; the positive charge can be located on either the C or the N atom. The C<sub>9</sub>–N<sub>6</sub> bond length and the symmetry equivalent C<sub>9</sub>'–N<sub>6</sub>' bond length of 133.5(4) pm are slightly shorter than the other six bond lengths from the central guanidino C atom to the N atoms of the NMe<sub>2</sub> groups (av. value 134.6 pm). Thus, these two bonds exhibit an increased degree of  $\pi$  bonding, although the bond length is significantly longer than, for example, the 126.3(5) pm adopted for the C=N bond in [H<sub>2</sub>C=NMe<sub>2</sub>]<sup>+</sup>Br.<sup>[18]</sup> The plane defined by the C<sub>9</sub>, N<sub>5</sub> and N<sub>6</sub> atoms is almost perpendicular to the plane defined by the C<sub>9</sub>, N<sub>4</sub> and C<sub>3</sub> atoms, so that the C<sub>9</sub>–N<sub>6</sub> and C<sub>3</sub>–N<sub>4</sub>  $\pi$  bonds cannot really communicate in the crystalline phase. The structure thus suggests that the positive charge is to some degree located on the NMe<sub>2</sub> groups (in line with the mesomeric form on the right side of Scheme 3). Quantum chemical (B3LYP/SVP) calculations were carried out to obtain information about the singlet–triplet gap in 6<sup>2+</sup>. Interestingly, the B3LYP/SVP calculations predict the lowest-energy triplet state to exhibit an energy not more than 110.4 kJ mol<sup>-1</sup> above the singlet-energy ground term.

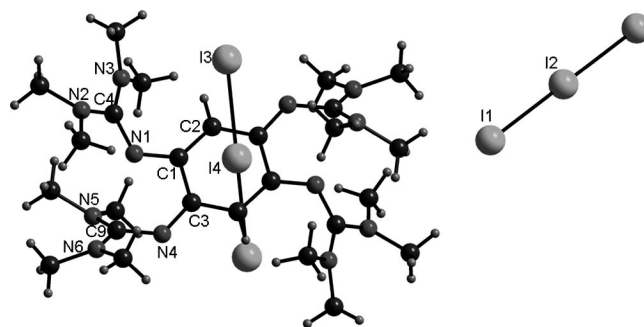


Figure 7. Molecular structure of 6(I<sub>3</sub>)<sub>2</sub>. Ellipsoids are drawn at the 50% probability level.

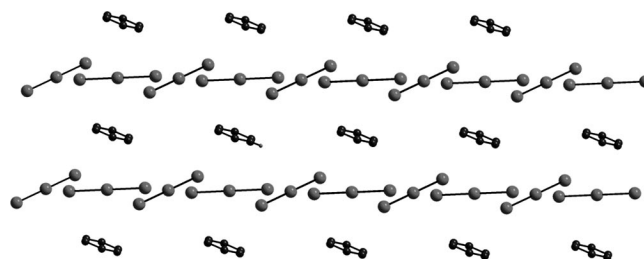
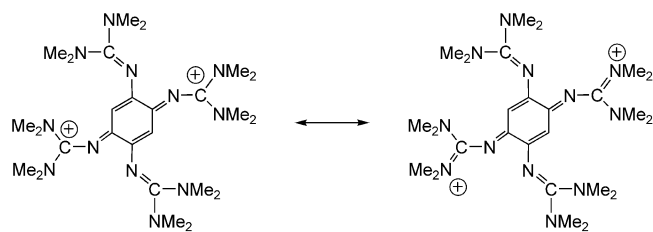
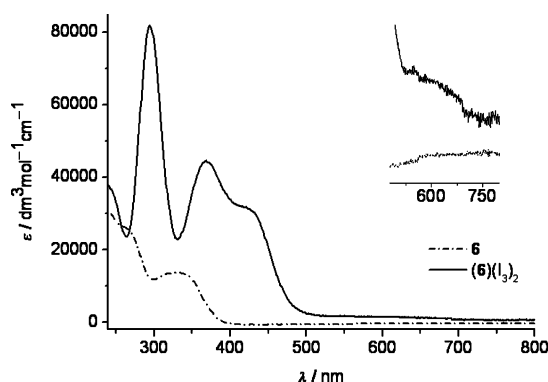


Figure 8. Layers of I<sub>3</sub><sup>-</sup> and bisguanidines (only the benzene rings are shown for the sake of clarity) in crystalline 6(I<sub>3</sub>)<sub>2</sub>.



Scheme 3.

The UV/Vis spectrum of  $\text{CH}_3\text{CN}$  solutions of  $\mathbf{6}(\text{I}_3)_2$  is displayed in Figure 9. Three strong absorptions are centred at 294, 367 and 422 nm. In addition, a broad and very weak band or family of bands was visible in the region 500–680 nm (see the inset in Figure 9). Solutions of the  $\text{I}_3^-$  anion formed by reaction between  $\text{I}_2$  and  $(n\text{-C}_4\text{H}_9)_4\text{NI}$  in  $\text{CH}_3\text{CN}$  were shown to exhibit strong absorptions at 292 and 363 nm (with extinction coefficients of 45900 and 25400  $\text{L mol}^{-1}\text{cm}^{-1}$ ) and an extremely weak one at 531 nm (with an extinction coefficient of not more than 155  $\text{L mol}^{-1}\text{cm}^{-1}$ ).<sup>[19]</sup> If the  $\text{I}_3^-$  anions were formed in solutions of  $\text{I}_2$  and KI in 0.050 M KI and 0.010 M  $\text{HClO}_4$ , the band positions (now 287, 353 and 535 nm) and extinction coefficients (41400, 25300 and 144  $\text{L mol}^{-1}\text{cm}^{-1}$ ) vary slightly. A problem encountered in the determination of the precise extinction coefficient is the equilibrium between  $\text{I}_3^-$  and  $\text{I}_2 + \text{I}^-$  (around 15–20% of the  $\text{I}_3^-$  molecules dissociate). By comparison with the literature data, the bands at 294 and 367 nm in our experiments can be assigned unambiguously to  $\text{I}_3^-$ . The relative intensities of the two absorptions match well with the literature values. Because two  $\text{I}_3^-$  anions are present in each of the formula units of  $\mathbf{6}(\text{I}_3)_2$ , the measured extinction coefficients are about twice as high as those reported in the literature. The band at 422 nm can then be assigned to the  $\mathbf{6}^{2+}$  dication. Excitations in these regions were not observed for neutral  $\mathbf{6}$ , which is in line with the significant changes the  $\pi$  system is subjected to in the course of the two-electron oxidation. Figure 10 shows the spectra recorded for oxidation of a  $\text{CH}_2\text{Cl}_2$  solution of  $\mathbf{6}$  with  $\text{O}_2$  from the air for several exposure times  $t$ . Note that evaporated  $\text{CH}_2\text{Cl}_2$  was not compensated to avoid any extra influence. Therefore, the extinction coefficient is strictly only correct at  $t = 0$ . The initial spectrum showed

Figure 9. UV/Vis spectra of  $\mathbf{6}$  and  $\mathbf{6}(\text{I}_3)_2$  dissolved in  $\text{CH}_3\text{CN}$ .

the band at 329 nm characteristic of neutral  $\mathbf{6}$ . This band decreased with increasing exposure times, and at the same time two new bands appeared centred at 422 and 615 nm. The band at 615 nm reached its maximum after an exposure time of  $t = 2\text{--}4$  h, and was almost extinguished again after  $t = 3$  d. The spectrum recorded after 3 d showed a strong band at 422 nm. Thus, it resembled the spectrum taken for  $\mathbf{6}(\text{I}_3)_2$ , but without the bands due to  $\text{I}_3^-$  at 294 and 367 nm. Consequently it can be concluded that the solution contained dication  $\mathbf{6}^{2+}$  after 3 d of air exposure.

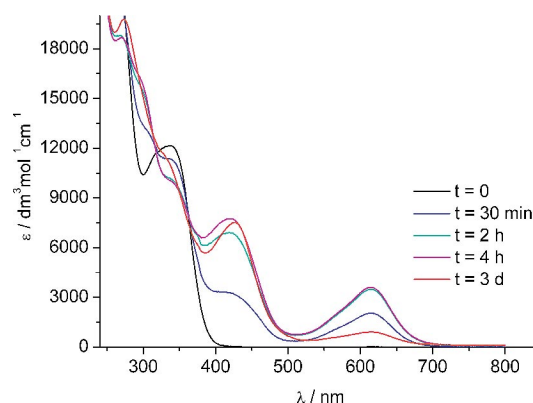


Figure 10. UV/Vis spectra recorded for a solution of  $\mathbf{6}$  in  $\text{CH}_2\text{Cl}_2$  at several exposure times to the air dioxygen molecules. Note that the evaporation of the solvent was not compensated for to avoid any potential extra influence. Therefore, the extinction coefficient is strictly only correct at the start.

### Comparison of the Donor Strength on the Basis of Quantum Chemical Calculations

Some additional quantum chemical calculations (B3LYP/SVP) on  $\mathbf{6}$  and other known organic electron-donor molecules were carried out. The performance of the calculations was tested by comparing calculated values with experimentally determined structural parameters. The calculated structures are visualised in Figure 11 (optimised coordinates can be found in the Supporting Information). In agreement with the experimental results, the benzene rings in dications  $\mathbf{1}^{2+}$  and  $\mathbf{2}^{2+}$  are folded, in clear contrast to the situation in  $\mathbf{6}^{2+}$ . The C–C distances within the  $\text{C}_6$  ring in  $\mathbf{2}^{2+}$  were calculated to be 141.0 and 151.0 pm. These values compare with experimentally obtained ones of 138.2(5) and 152.9(8) pm. As already mentioned, tetraazafulvalene  $\mathbf{4}$  (see Scheme 1) was shown to be an excellent reducing agent (organic “sodium”). The minimum structure as calculated with B3LYP/SVP is characterised by a central C=C bond length of 135.6 pm and an average distance of 142.2 pm between one of the two central C atoms and one of the four N atoms. These values are in good agreement to the experimental ones. Thus, the experimentally derived central C=C bond length in the neutral molecule is 133.7(5) pm and the experimental average C–N distance is 142.9(4) pm according to X-ray diffraction analysis.<sup>[8]</sup> They also agree with previous calculations using the gradient-corrected BP86 method and a def2-TZVP basis set resulting in values of

136 and 144 pm for the central C=C distance in the neutral and dicationic molecule, respectively.<sup>[10]</sup> As anticipated, the central C–C bond length (now being a single bond) increases in dication  $4^{2+}$  to 144.0 pm, whereas the central C–N distances decrease to 134.9 pm.

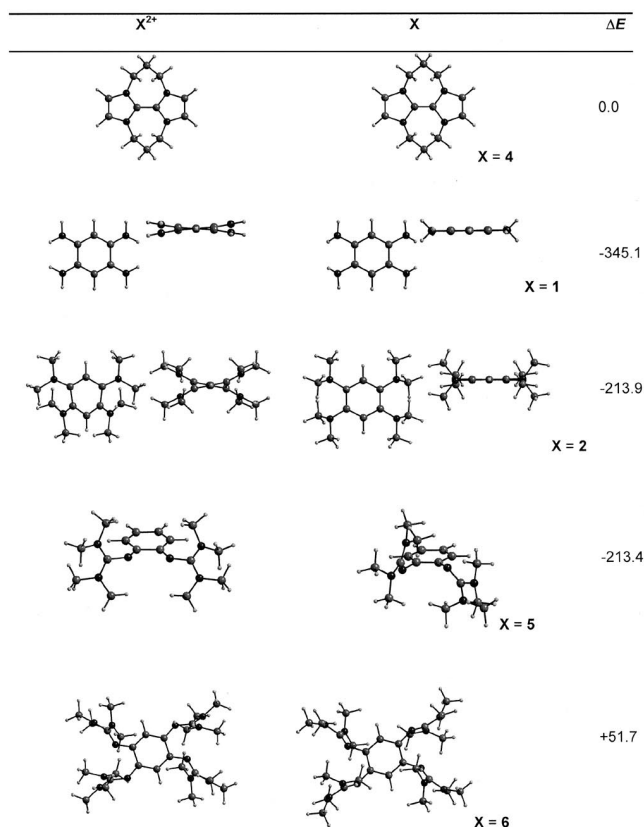


Figure 11. Energy changes  $\Delta E$  (in  $\text{kJ mol}^{-1}$ ) for the gas-phase redox reaction  $4 + X^{2+} \rightarrow 4^{2+} + X$  as calculated with B3LYP/SVP for different molecules X.

Figure 11 includes the gas-phase reaction energies for two-electron transfer from compound **4** to the dication of several relevant molecular electron donors X (see Equation 1 with X = **6**). The value of  $\Delta E$  comes out to be negative for X = **1**, **2** and **5**, but it turns positive for X = **6**. However, a comparison of the donor strength of course should be based on the Gibbs free energy rather than on the energies and should also consider solvent effects. We therefore first calculated the change in the standard reaction Gibbs free energy (at 298 K, 1 bar) for the redox reaction between **4** and  $6^{2+}$ . According to our calculations,  $\Delta G^0$  for the gas-phase reaction is  $62.0 \text{ kJ mol}^{-1}$ . Although this value shows that **6** is indeed a better two-electron donor than **4** in the gas-phase (neglecting any differences in the activation barriers for electron transfer, which certainly exist), the situation changes in solution. The shapes and sizes of **4** and **6** are quite different, leading to a large difference in the stabilisation of the dication in solution as modelled by the COSMO model. For DMF with a dielectric constant  $\epsilon = 38.2 \text{ L mol}^{-1} \text{ cm}^{-1}$ , we obtained  $\Delta_{\text{solv}} G^0 = -157.1 \text{ kJ mol}^{-1}$ . This means that in DMF solutions com-

pound **4** is a better two-electron donor than **6**, in agreement with the observed order of the  $E_{1/2}$  values in the CV experiments. For a solvent of  $\epsilon = 10 \text{ L mol}^{-1} \text{ cm}^{-1}$ , the calculations still returned  $\Delta_{\text{solv}} G^0 = -130.1 \text{ kJ mol}^{-1}$ . A dielectric constant  $\epsilon$  of less than about 3 is necessary to get to positive standard reaction Gibbs free energies, highlighting the dominating influence of the solvent on the reduction power of these species. Only in a weakly polar solvent (e.g., toluene  $\epsilon = 2.4 \text{ L mol}^{-1} \text{ cm}^{-1}$ ; 1,4-dioxane  $\epsilon = 2.3 \text{ L mol}^{-1} \text{ cm}^{-1}$ ) can compound **6** be expected to be a better two-electron reducing agent than **4**, whereas in higher polar solvents **4** should be superior. Of course, in practice the low solubility of the substrates in less-polar solvents limits the choice of solvent.

## Conclusions

This work deals with the synthesis and characterisation of a new molecular electron donor, namely 1,2,4,5-tetrakis-(tetramethylguanidino)benzene (ttmgb). Titration of ttmgb with HCl in water solutions led to several colour changes, starting with a yellow-coloured solution prior to HCl addition. Thus, solutions of the di- and tetraprotonated molecules are green and blue coloured, respectively. All colour changes are fully reversible. The molecular structures of the di- and tetraprotonated ttmgb molecule show that protonation occurs exclusively at the imine N atoms. The variation in the three CN bond lengths within each guanidino group shrink significantly upon protonation, which indicates delocalisation of the positive charge through extended  $\pi$  interactions. Whereas the electronic situation within the guanidino groups changes, the  $C_6$  ring remains aromatic and is only very slightly affected by protonation.

Oxidation of ttmgb (which already occurs with atmospheric  $O_2$ ) was followed by various spectroscopic techniques and by X-ray diffraction. Oxidation of ttmgb with  $I_2$  leads to  $(\text{ttmgb})(I_3)_2$ . The C–C distances within the  $C_6$  ring of this dication vary significantly, signalling the loss of aromaticity. At the same time, two of the four C–N distances involving the ring C atoms decrease. The rearrangement of the  $\pi$  system is also evident from the changes in the UV/Vis spectrum upon oxidation. The oxidised form is stabilised by formation of an extended  $\pi$  system. Quantum chemical calculations indicate that ttmgb could even reduce the dication of the “organic sodium” tetraazafulvalene (two-electron reduction) in the gas phase. However, the situation changes in polar solutions. The large and bulky dication  $(\text{ttmgb})^{2+}$  is significantly less stabilised by the solvent environment in comparison to the dication of tetraazafulvalene, which makes tetraazafulvalene a better two-electron donor than ttmgb in solutions with a dielectric constant larger than ca. 3. The new tetraguanidine ttmgb should have interesting properties not only in redox reactions as a mild reducing agent but also when used as a ligand in di- or oligonuclear paramagnetic complexes. In future studies we especially seek to explore ferromagnetic interactions through the phenylene bridge<sup>[20]</sup> in dinuclear ttmgb transition-metal complexes.

## Experimental Section

**General:** All synthetic work was carried out by using standard Schlenk techniques. UV/Vis spectra were recorded with a Perkin–Elmer Lambda spectrometer. An EG&G Princeton 273 apparatus was used for the CV measurements. IR spectra were taken with the help of a BIORAD Excalibur FTS 3000 spectrometer. NMR spectra were measured with a Bruker Avance II 400 spectrometer.

**6:** To a solution of *N,N,N',N'*-tetramethylurea (1.1 mL, 9.4 mmol) dissolved in dry  $\text{CHCl}_3$  (6 mL) was added oxalyl chloride (4 mL, 46.5 mmol, 4.9 equiv.) dropwise. The reaction mixture was stirred for 16 h under reflux. Then, the solvent was removed in vacuo. The remaining solid, 2-chloro-1,1',3,3'-tetramethylformamidium chloride, was washed with  $\text{Et}_2\text{O}$ , dissolved in  $\text{CH}_3\text{CN}$  (24 mL) and added slowly and dropwise to a  $\text{CH}_3\text{CN}$  solution (10 mL) containing 1,2,4,5-tetraaminobenzene (0.5 g, 1.8 mmol) and triethylamine (3.4 mL, 24.6 mmol) at a temperature of 0 °C. Subsequently, the mixture was stirred for an additional period of 1 h at 0 °C. The precipitate was filtered before being redissolved in HCl (10%). After addition of NaOH (20%), the solution was extracted with toluene (3×). The combined toluene phase was dried with  $\text{K}_2\text{CO}_3$ , and toluene was removed under vacuum to afford ttmgb (0.5683 g, 1.1 mmol, 61%) as a pale yellow-white solid. Upon recrystallisation from  $\text{CH}_3\text{CN}$  colourless crystals of ttmgb were obtained.  $^1\text{H}$  NMR (199.92 MHz,  $\text{CD}_3\text{CN}$ ):  $\delta$  = 5.54 (s, 2 H), 2.63 (s, 48 H,  $\text{CH}_3$ ) ppm.  $^1\text{H}$  NMR (399.89 MHz,  $\text{C}_6\text{D}_6$ ):  $\delta$  = 6.26 (s, 2 H), 2.66 (s, 48 H,  $\text{CH}_3$ ) ppm.  $^{13}\text{C}$  NMR (50.28 MHz,  $\text{CD}_3\text{CN}$ ):  $\delta$  = 158.27, 138.08, 115.58 (CH), 39.78 ( $\text{CH}_3$ ) ppm.  $^{13}\text{C}$  NMR (100.56 MHz,  $\text{C}_6\text{D}_6$ ):  $\delta$  = 157.23, 138.09, 115.76 (CH), 39.70 ( $\text{CH}_3$ ) ppm. IR (CsI):  $\tilde{\nu}$  = 3001 (w), 2923 (w), 2871 (w), 2801 (w), 1597 (vs), 1498 (s), 1477 (s), 1459 (s), 1422 (s), 1372 (vs), 1235 (s), 1137 (vs), 1062 (w), 1020 (s), 878 (s), 803 (w), 787 (w), 754 (w), 727 (w), 683 (w), 664 (w), 556 (w)  $\text{cm}^{-1}$ . UV/Vis ( $\text{CH}_3\text{CN}$ ,  $c$  =  $3.0 \times 10^{-5}$  mol  $\text{L}^{-1}$ ):  $\lambda_{\text{max}}$  ( $\epsilon$ ,  $\text{L mol}^{-1} \text{cm}^{-1}$ ) = 218 ( $3.93 \times 10^4$ ), 329 ( $1.36 \times 10^4$ ) nm. MS (FAB):  $m/z$  (%) = 532 (43) [(ttmgb)(H) $_2$ ] $^+$ , 531 (100) [(ttmgb)(H)] $^+$ , 530 (64) [ttmgb], 486 (41) [ttmgb-N( $\text{CH}_3$ ) $_2$ ]. Crystal data for **6**:  $\text{C}_{26}\text{H}_{50}\text{N}_{12}$ ,  $M_r$  = 530.78,  $0.40 \times 0.30 \times 0.30$  mm $^3$ , triclinic, space group  $P\bar{1}$ ,  $a$  = 8.1570(16) Å,  $b$  = 8.8210(18) Å,  $c$  = 11.337(2) Å,  $\alpha$  = 89.22(3)°,  $\beta$  = 85.08(3)°,  $\gamma$  = 74.13(3)°,  $V$  = 781.7(3) Å $^3$ ,  $Z$  = 1,  $d_{\text{calcd.}}$  = 1.128 Mg  $\text{m}^{-3}$ , Mo- $K_{\alpha}$  radiation (graphite monochromated,  $\lambda$  = 0.71073 Å),  $T$  = 200 K,  $\theta_{\text{range}}$  2.40 to 30.0°. Reflections measured 38438, independent 4537,  $R_{\text{int}}$  = 0.0366. Final  $R$  indices [ $I > 2\sigma(I)$ ]:  $R_1$  = 0.0504,  $wR_2$  = 0.1256.

**[6H $_4$ ]Cl $_4$ :** To a solution of **6** (0.06 g, 1.1 mmol) dissolved in  $\text{Et}_2\text{O}$  (10 mL) was added  $\text{Et}_2\text{O} \cdot \text{HCl}$  (1 M, 0.4 mL). After stirring for 30 min at room temperature the solvent was removed in vacuo. The remaining white solid product was recrystallised from  $\text{CH}_3\text{CN}$ .  $^1\text{H}$  NMR (399.89 MHz,  $\text{CD}_3\text{CN}$ ):  $\delta$  = 9.81 (s, 4 H), 6.66 (s, 2 H), 2.99 (s, 48 H,  $\text{CH}_3$ ) ppm.  $^{13}\text{C}$  NMR (100.56 MHz,  $\text{CD}_3\text{CN}$ ):  $\delta$  = 159.64, 130.16, 118.67 (CH), 41.39 ( $\text{CH}_3$ ) ppm. MS (FAB):  $m/z$  (%) = 532 (32) [(ttmgb)(H) $_2$ ] $^+$ , 531 (95) [(ttmgb)(H)] $^+$ , 530 (28) [ttmgb], 486 (50) [ttmgb-N( $\text{CH}_3$ ) $_2$ ], 408 (67), 379 (100), 260 (25), 202 (36). Crystal data for **[6H $_4$ ]Cl $_4$ ·9H $_2$ O**:  $\text{C}_{26}\text{H}_{54}\text{N}_{12}\text{Cl}_4 \cdot 9\text{H}_2\text{O}$ ,  $M_r$  = 1677.52,  $0.40 \times 0.30 \times 0.30$  mm $^3$ , monoclinic, space group  $C2/c$ ,  $a$  = 23.226(5) Å,  $b$  = 11.823(2) Å,  $c$  = 15.802(3) Å,  $\beta$  = 94.48(3)°,  $V$  = 4326.0(15) Å $^3$ ,  $Z$  = 4,  $d_{\text{calcd.}}$  = 1.288 Mg  $\text{m}^{-3}$ , Mo- $K_{\alpha}$  radiation (graphite monochromated,  $\lambda$  = 0.71073 Å),  $T$  = 200 K,  $\theta_{\text{range}}$  1.76 to 35.00°. Reflections measured 106531, independent 9486,  $R_{\text{int}}$  = 0.0555. Final  $R$  indices [ $I > 2\sigma(I)$ ]:  $R_1$  = 0.0415,  $wR_2$  = 0.0977.

**[6H $_2$ ](PF $_6$ ) $_2$ :** A mixture of **6** (0.030 g, 0.06 mmol) and  $[\text{NH}_4]\text{PF}_6$  (0.016 g, 0.1 mmol) in  $\text{CH}_3\text{CN}$  (20 mL) was stirred for 30 min at a temperature of 50 °C. After evaporation of the solvent, the remaining solid was redissolved in  $\text{CH}_3\text{CN}$ . Then, a small amount of char-

coal was added, and the solution was stirred for 10 min before being filtered through silica. After removal of the solvent in vacuo a green-yellow solid remained, which was redissolved in  $\text{CH}_2\text{Cl}_2$ . Yellow needles of **[6H $_2$ ](PF $_6$ ) $_2$**  (0.017 g, 0.021 mmol, 42%) precipitated from a solution of  $\text{CH}_2\text{Cl}_2/\text{Et}_2\text{O}$  (1:1).  $^1\text{H}$  NMR (399.89 MHz,  $\text{CD}_2\text{Cl}_2$ ):  $\delta$  = 6.11 (s, 2 H), 2.78 (s, 48 H,  $\text{CH}_3$ ) ppm.  $^{13}\text{C}$  NMR (100.56 MHz,  $\text{CD}_2\text{Cl}_2$ ):  $\delta$  = 40.24 ( $\text{CH}_3$ ) ppm. MS (FAB):  $m/z$  (%) = 676 (43) [(ttmgb)(H) $_2$ (PF $_6$ )] $^+$ , 531 (100) [(ttmgb)(H)] $^+$ , 486 (40) [(ttmgb - N( $\text{CH}_3$ ) $_2$ )]. Crystal data for **[6H $_2$ ](PF $_6$ ) $_2$ ·1.5H $_2$ O**:  $\text{C}_{26}\text{H}_{52}\text{N}_{12}\text{P}_2\text{F}_{12} \cdot 1.5\text{H}_2\text{O}$ ,  $M_r$  = 848.75,  $0.40 \times 0.25 \times 0.25$  mm $^3$ , monoclinic, space group  $P2_1/n$ ,  $a$  = 7.8380(16) Å,  $b$  = 21.349(4) Å,  $c$  = 12.478(3) Å,  $\beta$  = 105.90(3)°,  $V$  = 2008.1(7) Å $^3$ ,  $Z$  = 2,  $d_{\text{calcd.}}$  = 1.400 Mg  $\text{m}^{-3}$ , Mo- $K_{\alpha}$  radiation (graphite monochromated,  $\lambda$  = 0.71073 Å),  $T$  = 200 K,  $\theta_{\text{range}}$  1.95 to 27.50°. Reflections measured 64704, independent 4526,  $R_{\text{int}}$  = 0.0426. Final  $R$  indices [ $I > 2\sigma(I)$ ]:  $R_1$  = 0.0689,  $wR_2$  = 0.1801 ppm.

**6(I $_3$ ) $_2$ :** To a solution of **6** (0.0314 g, 0.06 mmol) in  $\text{CH}_3\text{CN}$  (20 mL) was added  $\text{I}_2$  (0.0313 g, 0.12 mmol). The solution turned deep-green in colour, from which purple-black crystals of **6(I $_3$ ) $_2$**  (0.0126 g, 0.01 mmol, 17%) of a metal appearance precipitated.  $^1\text{H}$  NMR (200.13 MHz,  $\text{CD}_3\text{CN}$ ):  $\delta$  = 5.17 (s, 2 H), 2.88 (s, 48 H,  $\text{CH}_3$ ) ppm.  $^{13}\text{C}$  NMR (100.56 MHz,  $\text{CD}_3\text{CN}$ ):  $\delta$  = 41.00 ( $\text{CH}_3$ ) ppm. IR (CsI):  $\tilde{\nu}$  = 2921 (w), 1597 (s), 1539 (s), 1501 (vs), 1466 (s), 1420 (s), 1399 (vs), 1315 (m), 1250 (s), 1231 (s), 1157 (vs), 1067 (w), 1020 (s), 897 (w), 840 (w), 810 (w), 752 (w), 687 (w), 623 (w), 549 (w)  $\text{cm}^{-1}$ . UV/Vis ( $\text{CH}_3\text{CN}$ ,  $c$  =  $1.1 \times 10^{-5}$  mol  $\text{L}^{-1}$ ):  $\lambda_{\text{max}}$  ( $\epsilon$ ,  $\text{L mol}^{-1} \text{cm}^{-1}$ ) = 215 ( $5.47 \times 10^4$ ), 295 ( $8.17 \times 10^4$ ), 369 ( $4.46 \times 10^4$ ) nm. MS (FAB):  $m/z$  (%) = 531 (8) [(ttmgb)(H)] $^+$ , 460 (12), 408 (30), 291 (49), 273 (9), 212 (25). Crystal data for **6(I $_3$ ) $_2$** :  $\text{C}_{26}\text{H}_{50}\text{N}_{12}\text{I}_6$ ,  $M_r$  = 1292.18,  $0.25 \times 0.25 \times 0.25$  mm $^3$ , triclinic, space group  $P\bar{1}$ ,  $a$  = 8.1920(16) Å,  $b$  = 9.6060(19) Å,  $c$  = 13.928(3) Å,  $\alpha$  = 108.13(3)°,  $\beta$  = 91.51(3)°,  $\gamma$  = 96.60(3)°,  $V$  = 1032.5(4) Å $^3$ ,  $Z$  = 1,  $d_{\text{calcd.}}$  = 2.078 Mg  $\text{m}^{-3}$ , Mo- $K_{\alpha}$  radiation (graphite monochromated,  $\lambda$  = 0.71073 Å),  $T$  = 200 K,  $\theta_{\text{range}}$  1.54 to 30.00°. Reflections measured 24847, independent 5922,  $R_{\text{int}}$  = 0.0251. Final  $R$  indices [ $I > 2\sigma(I)$ ]:  $R_1$  = 0.0332,  $wR_2$  = 0.0804.

**X-ray Crystallographic Study:** Suitable crystals were taken directly out of the mother liquor, immersed in perfluorinated polyether oil and fixed on top of a glass capillary. Measurements were made with a Nonius-Kappa CCD diffractometer with low-temperature unit by using graphite-monochromated Mo- $K_{\alpha}$  radiation. The temperature was set to 200 K. The data collected were processed by using the standard Nonius software.<sup>[21]</sup> All calculations were performed by using the SHELXT-PLUS software package. Structures were solved by direct methods with the SHELXS-97 program and refined with the SHELXL-97 program.<sup>[22,23]</sup> Graphical handling of the structural data during solution and refinement was performed with XPMA.<sup>[24]</sup> Atomic coordinates and anisotropic thermal parameters of non-hydrogen atoms were refined by full-matrix least-squares calculations. CCDC-699399 (for **6**), -699401 (for **[6H $_4$ ]Cl $_4$ ·9H $_2$ O**), -699402 (for **[6H $_2$ ](PF $_6$ ) $_2$ ·1.5H $_2$ O**) and -699400 (**6(I $_3$ ) $_2$** ) contain the supplementary crystallographic data for this paper. These data can be obtained free of charge from The Cambridge Crystallographic Data Centre via [www.ccdc.cam.ac.uk/data\\_request/cif](http://www.ccdc.cam.ac.uk/data_request/cif).

**Details of the Quantum Chemical Calculations:** Calculations were carried out with the aid of the TURBOMOLE program package<sup>[25]</sup> Pure DFT calculations relied on the hybrid method B3LYP (DFT by using Becke exchange functional and Lee–Yang–Parr correlation functional, as well as Hartree–Fock exchange).<sup>[26]</sup> Calculations on the solvent effect were carried out with the COSMO program.<sup>[27]</sup>

**Supporting Information** (see footnote on the first page of this article): Selected structural parameters (bond lengths and angles) for **6**,  $[6H_4]Cl_4 \cdot 9H_2O$ ,  $[6H_2](PF_6)_2 \cdot 1.5H_2O$  and  $6(I_3)_2$ ; optimised energies and coordinates from B3LYP/SVP calculations and vibrational properties (from BP86/SVP calculations and only for compounds **4** and **6**) for several molecular electron donors and their oxidised forms.

## Acknowledgments

Continuous financial support from the Deutsche Forschungsgemeinschaft is gratefully acknowledged. We thank Monica Fuchs and Matthias Reinmuth for their help with some data collection.

- [1] a) C. Wurster, *Ber. Dtsch. Chem. Ges.* **1879**, *12*, 2071–2073; b) C. Wurster, E. Schobig, *Ber. Dtsch. Chem. Ges.* **1879**, *12*, 1807–1813; c) R. Kuhn, H. Katz, *Z. Angew. Chem.* **1933**, *46*, 478–479.
- [2] a) R. Nietzki, E. Hagenbach, *Ber. Dtsch. Chem. Ges.* **1887**, *20*, 328–332; b) R. Nietzki, *Z. Angew. Chem.* **1887**, *20*, 2114–2121; c) R. Nietzki, E. Müller, *Z. Angew. Chem.* **1889**, *22*, 440; d) P. Ruggli, R. Fischer, *Helv. Chim. Acta* **1945**, *28*, 1270–1280.
- [3] K. Elbl, C. Krieger, H. A. Staab, *Angew. Chem.* **1986**, *98*, 1024–1026; *Angew. Chem. Int. Ed. Engl.* **1986**, *25*, 1023–1025.
- [4] a) B. Speiser, M. Würde, C. Maichle-Mössmer, *Chem. Eur. J.* **1998**, *4*, 222–233; b) J. M. Chance, B. Kahr, A. B. Buda, J. P. Toscano, K. Mislow, *J. Org. Chem.* **1988**, *53*, 3226–3232; c) M. Dietrich, J. Heinze, *J. Am. Chem. Soc.* **1990**, *112*, 5142–5145; d) B. Speiser, M. Würde, M. G. Quintanilla, *Electrochem. Commun.* **2000**, *2*, 65–68.
- [5] H. A. Staab, A. Kirsch, T. Barth, C. Krieger, F. A. Neugebauer, *Eur. J. Inorg. Chem.* **2000**, 1617–1622.
- [6] O. Siri, P. Braunstein, M.-M. Rohmer, M. Bénard, R. Welter, *J. Am. Chem. Soc.* **2003**, *125*, 13793–13803.
- [7] O. Siri, P. Braunstein, *Chem. Commun.* **2000**, 2223–2224.
- [8] T. A. Taton, P. Chen, *Angew. Chem.* **1996**, *108*, 1098–1100; *Angew. Chem. Int. Ed. Engl.* **1996**, *35*, 1011–1013.
- [9] F. Schoenebeck, J. A. Murphy, S.-ze Zhou, Y. Uenoyama, Y. Miclo, T. Tuttle, *J. Am. Chem. Soc.* **2007**, *129*, 13368–13369.
- [10] J. A. Murphy, S.-ze Zhou, D. W. Thomson, F. Schoenebeck, M. Mahesh, S. R. Park, T. Tuttle, L. E. A. Berlouis, *Angew. Chem.* **2007**, *119*, 5270–5275; *Angew. Chem. Int. Ed.* **2007**, *46*, 5178–5183.
- [11] R. D. Richardson, T. Wirth, *Chem. Unserer Zeit* **2008**, *42*, 186–191.
- [12] G. P. McGlacken, T. A. Khan, *Angew. Chem.* **2008**, *120*, 1843–1847; *Angew. Chem. Int. Ed.* **2008**, *47*, 1819–1823.
- [13] See, for example: a) W. W. Porter III, T. P. Vaid, A. L. Rheingold, *J. Am. Chem. Soc.* **2005**, *127*, 16559–16566; b) J. A. Murphy, J. Garnier, S. R. Park, F. Schoenebeck, S.-ze Zhou, A. T. Turner, *Org. Lett.* **2008**, *10*, 1227–1230.
- [14] A. Peters, U. Wild, O. Hübner, E. Kaifer, J. Mautz, H.-J. Himmel, *Chem. Eur. J.* **2008**, *14*, 7813–7821.
- [15] V. Raab, J. Kipke, R. M. Gschwind, J. Sundermeyer, *Chem. Eur. J.* **2002**, *8*, 1682–1693.
- [16] U. Wild, O. Hübner, A. Maronna, M. Enders, E. Kaifer, H. Wadepohl, H.-J. Himmel, *Eur. J. Inorg. Chem.* **2008**, 4440–4447.
- [17] R. P. Thummel, V. Goulle, B. Chen, *J. Org. Chem.* **1989**, *54*, 3057–3061.
- [18] G. R. Clark, G. L. Shaw, P. W. J. Surman, M. J. Taylor, *J. Chem. Soc. Faraday Trans.* **1994**, *90*, 3139–3144.
- [19] H. Isci, W. R. Mason, *Inorg. Chem.* **1985**, *24*, 271–274.
- [20] M. Mitani, D. Yamaki, Y. Takano, Y. Kitagawa, Y. Yoshioka, K. Yamaguchi, *J. Chem. Phys.* **2000**, *113*, 10486–10504.
- [21] DENZO-SMN, Data Processing Software, Nonius, **1998**; <http://www.noniuss.com>.
- [22] a) G. M. Sheldrick, *SHELXS-97, Program for Crystal Structure Solution*, University of Göttingen, **1997**; <http://shelx.uni-ac.gwdg.de/SHELX/index.html>; b) G. M. Sheldrick, *SHELXL-97, Program for Crystal Structure Refinement*, University of Göttingen, **1997**; <http://shelx.uni-ac.gwdg.de/SHELX/index.html>.
- [23] *International Tables for X-ray Crystallography*, Kynoch Press, Birmingham, U. K., **1974**, vol. 4.
- [24] L. Zsolnai, G. Huttner, *XPMA*, University of Heidelberg, **1994**; <http://www.uni-heidelberg.de/institute/fak12/AC/huttner/software/software.html>.
- [25] a) R. Ahlrichs, M. Bär, M. Häser, H. Horn, C. Kölmel, *Chem. Phys. Lett.* **1989**, *162*, 165–169; b) K. Eichkorn, O. Treutler, H. Öhm, M. Häser, R. Ahlrichs, *Chem. Phys. Lett.* **1995**, *240*, 283–289; c) K. Eichkorn, O. Treutler, H. Öhm, M. Häser, R. Ahlrichs, *Chem. Phys. Lett.* **1995**, *242*, 652–660; d) K. Eichkorn, F. Weigend, O. Treutler, R. Ahlrichs, *Theor. Chem. Acc.* **1997**, *97*, 119–124; e) F. Weigend, M. Häser, *Theor. Chem. Acc.* **1997**, *97*, 331–340; f) F. Weigend, M. Häser, H. Patzelt, R. Ahlrichs, *Chem. Phys. Lett.* **1998**, *294*, 143–152.
- [26] a) A. D. Becke, *J. Chem. Phys.* **1993**, *98*, 5648–5652; b) P. J. Stephens, F. J. Devlin, C. F. Chabalowski, M. J. Frisch, *J. Phys. Chem.* **1994**, *98*, 11623–11627.
- [27] A. Klamt, G. Schürmann, *J. Chem. Soc. Perkin Trans. 2* **1993**, 799–805.

Received: September 15, 2008

Published Online: October 31, 2008